Spin-orbit coupling in graphene induced by adatoms with outer-shell *p* orbitals

Luis Brey*

Departamento de Teoría y Simulación de Materiales, Instituto de Ciencia de Materiales de Madrid, CSIC, 28049 Cantoblanco, Spain

(Received 17 September 2015; revised manuscript received 23 November 2015; published 29 December 2015)

Many of the exotic properties proposed to occur in graphene rely on the possibility of increasing the spin-orbit coupling (SOC). By combining analytical and numerical tight-binding calculations, in this paper we study the SOC induced by heavy adatoms with active electrons living in *p* orbitals. Depending on the position of the adatoms on graphene, different kinds of SOC appear. Adatoms located in a hollow position induce spin-conserving intrinsiclike SOC, whereas a random distribution of adatoms induces a spin-flipping Rashba-like SOC. The induced SOC is linearly proportional to the adatom concentration, indicating the nonexistent interference effects between different adatoms. By computing the Hall conductivity, we have proven the stability of the topological quantum Hall phases created by the adatoms against inhomogeneous spin-orbit coupling. For the case of Pb adatoms, we find that a concentration of 0.1 adatoms per carbon atom generates SOC's of the order of ∼40 meV.

DOI: 10.1103/PhysRevB.92.235444 PACS number(s): 73.22.Pr

I. INTRODUCTION

Research on graphene, a two-dimensional crystal of carbon atoms, has led to the discovery of a large number of interesting electrical, magnetic, mechanical, and optical properties [1,2]. The small atomic number of carbon implies that electrical carriers in graphene have an extremely weak spin-orbit (SO) coupling [3,4]. This property in combination with the large graphene electron mobility makes graphene a very good candidate for using in spintronics [5,6].

On the other hand, some proposals of exotic topological phases in graphene rely on the possibility of increasing the SOC. Because of the graphene lattice symmetry, there are two types of spin-orbit coupling in graphene, *intrinsiclike*, where the $\hat{z}$ component of the electron spin is a good quantum number and *Rashba-like*, which mixes spins and appears in the absence of mirror symmetry [7]. In graphene, the intrinsic SOC opens a gap, and the system becomes a quantum spin-Hall insulator, with gapless edge states able to transport spin and charge [8,9]. Nontrivial topological phases may also occur in multilayer graphene [10]. Quantum anomalous Hall effect was predicted to occur in bilayer and monolayer graphene in the presence of Rashba SOC and an exchange field or magnetic impurities [11,12]. The experimental realization of these topological phases requires a large SOC, and therefore there is considerable interest [13–22] in increasing the SOC and clearing the way to the study of exotic topological phases in graphene. Experimental reports on enhancement of SOC in graphene by weak hydrogenation [17], gold hybridization [23], or proximity with WS_2 [19] indicate that it is possible to increase the SOC in almost three orders of magnitude. Recently, it has been reported that graphene grown on Cu shows a SO splitting around 20 meV [24]. Intercalation of Au atoms in graphene grown on Ni produces a SO splitting of near 100 meV [23]. Similarly, the intercalation of Pb atoms in graphene grown on an iridium substrate seems to produce a giant SOC [18]. Theoretically, it has been proposed that hydrogenated [25] or fluorinated [26,27] graphene can get a large induced SOC. It has also been proposed that heavy adatoms with partially filled *p* shells, deposited on symmetric positions of the graphene lattice, could induce large intrinsic SOC [28].

In this paper we study the SOC induced by heavy adatoms with active electrons living in *p* orbitals; in particular we consider Pb atoms that have been proven to induce large SO effects in graphene [18]. The physical picture is the following: The tunneling of an electron between two carbon atoms through the adatom *p* orbitals opens additional channels for hopping in graphene. The SOC between the adatom *p* orbitals makes that the tunneling channels can conserve the spin inducing an intrinsic SOC or can flip the spin inducing a Rashba-like SOC.

By combining analytical calculations, perturbation theory, and tight-binding-based numerical simulations, we study the type of SO coupling induced by adatoms residing in different positions of the graphene unit cell. In addition, we study how a finite density of adatoms, in different distributions, affects the induced SO couplings. The main conclusions of our paper are the following:

(i) Adatoms located in hollow positions, see Fig. 1, induce intrinsic SOC. A finite density of adatoms in hollow positions randomly distributed opens an energy gap at the Dirac points that increases linearly with the adatom concentration. This gapped phase is a quantum spin-Hall state. The simulations indicate that, even for high adatom coverage, there are not interference effects between the adatoms, and the gap only depends on adatom density. In the case of Pb atoms we find gaps of the order of 50 meV for a concentration of 0.1 adatom per carbon.

(ii) For adatoms placed in top positions, see Fig. 1, the tunneling from graphene to the adatom and back induces a Rashba-like spin-flip hopping between the underneath C atom and its first neighbors and an intrinsiclike spin-conserving second neighbors tunneling between the carbons surrounding the underneath carbon atom. The intrinsiclike SOC induced by adatoms in top positions has opposite sign from that induced by adatoms in hollow geometry. The Rashba SOC has the same sign independently of the sublattice of the underneath carbon.

(iii) A finite density of adatoms randomly distributed on graphene induces a finite Rashba SOC linearly proportional

*brey@icmm.csic.es

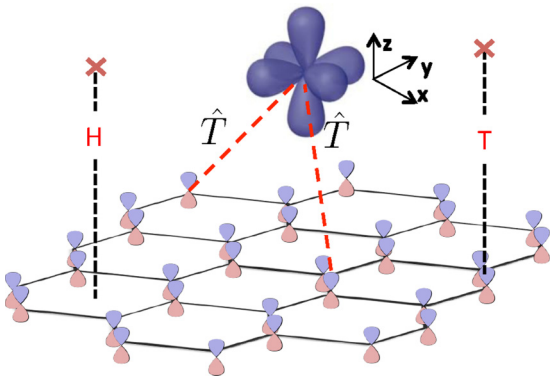

FIG. 1. (Color online) Schematic representation of the effective hopping between carbon atoms induced by an adatom with active electrons in outer p shells. Vertical H and T lines indicate the hollow and top positions, respectively.

to the density of adatoms. For a random distribution of adatoms, the resulting intrinsiclike SOC vanishes, because contributions from different locations of the adatoms have opposite signs. Similar results are obtained when the adatoms form an array commensurate with a large graphene supercell. By computing the Hall conductivity, we have obtained that a random distribution of adatoms on graphene in the presence of an exchange field is a quantum anomalous Hall system. When the adatom is Pb, we obtain that the Rashba SO coupling can be as large as 35 meV for a concentration of 0.1 Pb per carbon atom.

The rest of the paper is organized in the following way: In Sec. II we introduce the graphene and adatom Hamiltonians, and in Sec. III we describe the hopping between graphene carbon atoms and the adatom p orbitals. In Sec. IV we present the perturbation theory for describing the adatom mediated effective hopping between carbon atoms. The knowledge of the effective hopping between carbon atoms allows us to obtain, in Sec. V, analytical expressions for SOC induced by adatoms located in top and hollow positions. Section VI presents tight-binding-based numerical simulations for studying the effect that a random or commensurate distribution of adatoms have on the induced SOC. In Sec. VII we calculate the topological properties of graphene doped with adatoms. We close the paper with a summary of the results.

II. PRELIMINARIES

A. Graphene Hamiltonian

In graphene, carbon atoms crystallize in a triangular lattice of primitive translation vectors $\mathbf{a} = (0,a)$ and $\mathbf{b} = (\sqrt{3}/2,1/2)a$, where $a = 2.46$ Å is the lattice constant. The positions of the triangular lattices are $\mathbf{R}_i$. There are two atoms per unit cell located at positions $\mathbf{d}_A = (0,0)$ and $\mathbf{d}_B = (a/\sqrt{3},0)$ that define sublattices A and B in graphene. Covalent sp_2 bonds between carbon atoms stabilize this honeycomb lattice whereas the tunneling between p_z orbitals is the origin of the low energy active conduction and valence π bands. The band structure is rather well described by a tight-binding model with hopping $t \sim 2.7$ eV between first neighbors carbon p_z orbitals,

$$H_0 = -t \sum_{\langle i_A,i_B\rangle,\sigma} (|Z,i_A,\sigma\rangle\langle Z,i_B,\sigma| + \text{H.c.}). \tag{1}$$

Here the sum runs over first neighbor pairs, and $|Z,i_\alpha,\sigma\rangle$ represents the wave function of an electron at position $\mathbf{R}_i + \mathbf{d}_\alpha$ occupying a carbon p_z orbital with z component of the spin σ. The energy of the p_z carbon orbital is chosen as the zero of energies.

In graphene the intrinsic SOC has a chiral structure of the form

$$H^I_{\text{SO}} = \lambda^{\text{SO}} \sum_{\langle i_\alpha,j_\alpha\rangle,\sigma} \left(i\sigma\left(\hat{\mathbf{u}}_{i_\alpha} \times \hat{\mathbf{u}}_{j_\alpha}\right)_z |Z,i_\alpha,\sigma\rangle\langle Z,j_\alpha,\sigma| + \text{H.c.}\right), \tag{2}$$

where the sum runs over second nearest neighbor carbon atoms, and $\hat{\mathbf{u}}_{i_\alpha}$ is a unit vector parallel to $\mathbf{R_i} + \mathbf{d}_\alpha$. Note that the intrinsic SOC conserves spin, and it is not associated with broken mirror symmetry. On the contrary, Rashba SOC appears because of broken mirror symmetry, in particular due to the substrate, and induces a coupling between first neighbors with opposite spin of the form

$$H^R_{\text{SO}} = i\lambda^R \sum_{\langle i_A,j_B\rangle,\sigma,\sigma'} ((\boldsymbol{\sigma} \times \hat{\mathbf{u}}_{i_A j_B})_z |Z,i_A,\sigma\rangle\langle Z,j_B,\sigma'| + \text{H.c.}), \tag{3}$$

where $\hat{\mathbf{u}}_{i_\alpha j_\beta}$ is a unit vector parallel to $\mathbf{R}_j + \mathbf{d}_\beta - \mathbf{R}_i - \mathbf{d}_\alpha$ and $\boldsymbol{\sigma}$ the electron spin Pauli matrices.

In the absence of SO couplings the conduction and valence bands touch at two inequivalent points of the Brillouin zone $\mathbf{K} = (0, \frac{4\pi}{3a})$ and $\mathbf{K}' = (0, -\frac{4\pi}{3a})$ which are the celebrated Dirac points. Near these points the low energy physics is described by the Dirac equation

$$H_0 = \hbar v_F (k_x \sigma_0 \otimes \tau_x + s k_y \sigma_0 \otimes \tau_y), \tag{4}$$

where the moment $\mathbf{k}$ is measured with respect to the Dirac points, $s = 1$ and -1 stand for $\mathbf{K}$ and $\mathbf{K}'$, respectively, and $\boldsymbol{\tau}$ are the Pauli matrices acting on the spinor defined by the amplitude of the wave function on sublattices A and B. In the previous equation σ_0 represents the unity matrix in the spin sector. The Fermi velocity is related to the hopping through the relation $\hbar v_F = \frac{\sqrt{3}}{2} ta$. In this continuum approximation, and neglecting higher order terms in momentum $\mathbf{k}$ [29], the SO terms get the form

$$H^I_{\text{SO}} = 3\sqrt{3}\lambda^{\text{SO}} s \sigma_z \otimes \tau_z \tag{5}$$

$$H^R_{\text{SO}} = \frac{3}{2}\lambda^R (\sigma_y \otimes \tau_y + s\sigma_x \otimes \tau_x). \tag{6}$$

B. Adatom Hamiltonian

We consider heavy atoms with the active electrons living in p orbitals. The Hamiltonian describing the electrons in the adatom contains a spin-orbit coupling part and a crystal field H_{CF} term. In the basis$\{|p_x\uparrow\rangle, |p_y\uparrow\rangle, |p_z\uparrow\rangle, |p_x\downarrow\rangle, |p_y\downarrow\rangle,$

$|p_z\downarrow\rangle\}$ the Hamiltonian reads

$$H_p = \Delta_{\rm SO}\mathbf{L}\cdot\boldsymbol{\sigma} + H_{\rm CF} = \frac{\Delta_{\rm SO}}{2}\begin{pmatrix} 0 & -i & 0 & 0 & 0 & 1 \\ i & 0 & 0 & 0 & 0 & -i \\ 0 & 0 & 0 & -1 & i & 0 \\ 0 & 0 & -1 & 0 & i & 0 \\ 0 & 0 & -i & -i & 0 & 0 \\ 1 & i & 0 & 0 & 0 & 0 \end{pmatrix} + \begin{pmatrix} \epsilon_x & 0 & 0 & 0 & 0 & 0 \\ 0 & \epsilon_y & 0 & 0 & 0 & 0 \\ 0 & 0 & \epsilon_z & 0 & 0 & 0 \\ 0 & 0 & 0 & \epsilon_x & 0 & 0 \\ 0 & 0 & 0 & 0 & \epsilon_y & 0 \\ 0 & 0 & 0 & 0 & 0 & \epsilon_z \end{pmatrix}. \quad (7)$$

Here $\Delta_{\rm SO}$ is the spin-orbit coupling parameter, and $\mathbf{L}$ and $\boldsymbol{\sigma}$ are the usual angular momentum and spin operators. Nonspherical effects occurring in the geometry produce a crystal field that splits the energies of the p orbitals. For adatoms deposited on planar graphene, we expect that $\epsilon_x = \epsilon_y \neq \epsilon_z$.

III. TUNNELING BETWEEN AN ADATOM AND A CARBON Z ORBITAL

We consider an adatom placed at position $\mathbf{r} = (x,y,h)$, where h is the vertical distance between graphene and the adatoms, Fig. 2. The tunneling amplitudes between a carbon orbital located at position $\mathbf{R}_i = (X_i, Y_i, 0)$ and the adatom p_x, p_y, and p_z orbitals are

$$\begin{aligned} \langle Z,i,\sigma|\hat{T}|p_x,\sigma\rangle &= \tfrac{1}{2}\cos\phi\sin 2\theta(V_{pp\sigma}(d) - V_{pp\pi}(d)) \\ \langle Z,i,\sigma|\hat{T}|p_y,\sigma\rangle &= \tfrac{1}{2}\sin\phi\sin 2\theta(V_{pp\sigma}(d) - V_{pp\pi}(d)) \\ \langle Z,i,\sigma|\hat{T}|p_z,\sigma\rangle &= \cos^2\theta V_{pp\pi}(d) + \sin^2\theta V_{pp\sigma}(d), \end{aligned} \quad (8)$$

where $\theta = \tan^{-1}\frac{h}{\sqrt{(x-X_i)^2+(y-Y_i)^2}}$, $\phi = \tan^{-1}\frac{y-Y_i}{x-X_i}$, and $V_{pp\sigma}$ and $V_{pp\pi}$ are the Slater-Koster hopping parameters between the p_z graphene orbital and the heavy adatom p orbitals. The hopping parameters depend on the distance $d = \sqrt{(x-X_i)^2 + (y-Y_i)^2 + h^2}$ between the atoms that we parametrize in the form $V_{pp\sigma(\pi)}(d) = V_{pp\sigma(\pi)}(d=h)e^{-\beta(d-h)}$, with $\beta = 3$ [30] and $V_{pp\sigma(\pi)}(h)$ obtained from density functional calculations [18]. Note that in the tunneling process the carrier spin is conserved. Because of the symmetry of the p orbitals, the hopping amplitude between a carbon p_z orbital in graphene and the p_x and p_y adatom orbitals have opposite sign depending on whether the adatom is deposited on the top or bottom of the graphene sheet. On the contrary, the hopping between z orbitals is independent of the position of the adatom with respect to the graphene layer.

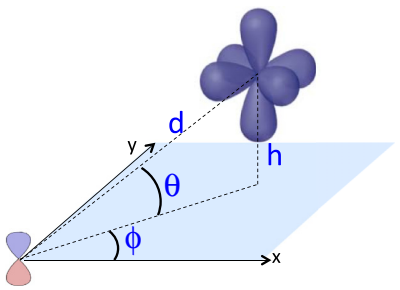

FIG. 2. (Color online) Geometry of an adatom located at a distance h of the graphene layer. The angles θ and ϕ and the distance d define the spherical coordinates of the adatom with respect to a carbon atom.

IV. TUNNELING BETWEEN CARBON ATOMS MEDIATED BY AN ADATOM

The spin-orbit coupling in the adatom located at $\mathbf{r} = (x,y,h)$ allows an extra path for tunneling between two carbon atoms located at $\mathbf{R}_i$ and $\mathbf{R}_j$ with spin σ and σ', respectively. In second order perturbation theory a single adatom produces a coupling between the carbon atoms of the form

$$\gamma_{i\sigma,j\sigma'} = \sum_l \frac{\langle Z,i,\sigma|\hat{T}|\tilde{p}_l\rangle\langle\tilde{p}_l|\hat{T}|Z,j,\sigma'\rangle}{\tilde{\epsilon}_l}, \quad (9)$$

here $|\tilde{p}_l\rangle$ and $\tilde{\epsilon}_l$ are the eigenfunctions and eigenvalues of Hamiltonian Eq. (7). Because of the form of spin-orbit coupling in the adatom outer p shell, the induced hoppings satisfy the following relations for $i \neq j$,

$$\begin{aligned} \gamma_{i\sigma,j-\sigma} &= -\gamma^*_{i-\sigma,j\sigma} \\ \gamma_{i\sigma,j\sigma} &= \gamma^*_{i-\sigma,j-\sigma} \\ \gamma_{i\sigma,j\sigma'} &= \gamma^*_{j\sigma',i\sigma}, \end{aligned} \quad (10)$$

and for $i = j$,

$$\gamma_{\ i\sigma,i\sigma} = \gamma_{i-\sigma,i-\sigma} \quad (11)$$

$$\gamma_{\ i\sigma,i-\sigma} = 0. \quad (12)$$

The adatom gives rise to two kind of SO assisted tunneling:
(i) spin-conserved tunneling events of the form

$$|Z,i,\sigma\rangle \xrightarrow{\hat{T}} |p_{x(y)}\sigma\rangle \xrightarrow{H_p} |p_{y(x)}\sigma\rangle \xrightarrow{\hat{T}} |Z,j,\sigma\rangle \quad (13)$$

that are pure imaginary and change sign when reversing spin. Following the standard notation we call it *intrinsic* spin-orbit coupling. This tunneling amplitude behaves as $\sin^2(2\theta)$; it is zero when the adatom is in the graphene sheet, being independent on the top or bottom position of the adatom with respect to the graphene layer.
(ii) nonconserving spin processes of the form

$$\begin{aligned} |Z,i,\sigma\rangle &\xrightarrow{\hat{T}} |p_z\sigma\rangle \xrightarrow{H_p} |p_{x(y)} - \sigma\rangle \xrightarrow{\hat{T}} |Z,j,-\sigma\rangle \\ |Z,i,\sigma\rangle &\xrightarrow{\hat{T}} |p_{x(y)}\sigma\rangle \xrightarrow{H_p} |p_z - \sigma\rangle \xrightarrow{\hat{T}} |Z,j,-\sigma\rangle. \end{aligned} \quad (14)$$

These terms get origin on the lack of mirror symmetry in the hopping between z orbitals, and we refer to this tunneling contribution as Rashba SOC. This tunneling amplitude behaves as $\sin(2\theta)$ and changes sign when the adatom is located on the top or the bottom of the graphene layer.

V. EFFECTIVE HAMILTONIANS FOR HOLLOW AND TOP POSITIONS

When the adatoms are located at high symmetry points of the graphene lattice, it is possible to write down analytic expressions for the effect that the SO induces on the graphene low energy band structure. The procedure consists of projecting the perturbation created by the adatom on the atomic Bloch states at the $\mathbf{K}$ and $\mathbf{K}'$ Dirac points,

$$\Psi_{A,s,\sigma} = \frac{1}{\sqrt{N}}\sum_i e^{is\mathbf{K}\mathbf{R}_i}|Z,i_A,\sigma\rangle$$
$$\Psi_{B,s,\sigma} = \frac{1}{\sqrt{N}}\sum_i e^{is\mathbf{K}\mathbf{R}_i}|Z,i_B,\sigma\rangle, \quad (15)$$

where N is the number of unit cells in the crystal. These Bloch states are the eigenstates of the Dirac Hamiltonian, Eq. (4) for $\mathbf{k}=0$. When the adatoms form a periodic array with a reciprocal lattice vector equal to an integer number of $\mathbf{K}-\mathbf{K}'$, there is a non-negligible coupling between states coming from different Dirac cones [31]. We avoid this situation by choosing appropriate coverages for which the valleys are separated in reciprocal space [31]. Under this condition, it is appropriate to assume that the adatoms do not induce coupling between states coming from different Dirac cones.

A. Adatom in hollow position

In the hollow geometry the adatom is located on top of the center of a hexagon of the graphene lattice at a height h, see Fig. 1. We consider SO induced tunneling up to third neighbors; tunneling between more distant atoms can be neglected because of the exponential decrease of the tunneling amplitude with the distance. Coupling between Bloch wave functions of different sublattices involves first and third neighbor hopping and gets the form

$$\langle\Psi_{A,s,\sigma}|V_H|\Psi_{|B,s,\sigma'}\rangle = \frac{1}{N}\sum_{i_A,j_B}\gamma_{i_A\sigma,j_B\sigma'}e^{is\mathbf{K}(\mathbf{R}_j-\mathbf{R}_i)}, \quad (16)$$

where i_A (j_B) runs over the vertices, of sublattice A (B), of the hexagon surrounding the adatom. V_H represents the perturbation created by the adatom in the hollow position.

The coupling between Bloch states of the same sublattice involves second neighbor tunneling and gets the form

$$\langle\Psi_{A,s,\sigma}|V_H|\Psi_{|A,s,\sigma'}\rangle = \frac{1}{N}\sum_{i_A\neq j_A}\gamma_{i_A\sigma,j_A\sigma'}e^{is\mathbf{K}(\mathbf{R}_j-\mathbf{R}_i)}. \quad (17)$$

A similar expression applies for $\langle\Psi_{B,s,\sigma}|V_H|\Psi_{|B,s,\sigma'}\rangle$. The adatom also induces diagonal self-energies that for the adatom in the hollow position are equal for both Dirac points, spin orientation, and graphene sublattices.

In the hollow geometry and for $\sigma'=-\sigma$, it is possible to sum the six terms, Eq. (14), that contribute to spin-flip effective tunneling, and we get

$$\gamma_{i\sigma,j-\sigma} = -\sigma t_R(e^{-i\sigma\phi_j}-e^{-i\sigma\phi_i}), \quad (18)$$

t_R being a constant that depends on the carbon to adatom tunneling parameters, Eq. (8). Using this expression and relations Eq. (10), we obtain that in the hollow position an adatom with outer shell p orbitals does not induce momentum independent nonconserving spin tunneling and therefore does not induce Rashba-like SOC in graphene.

For spin-conserving SO induced tunneling, the sum of the two processes described in Eq. (13) gives a hopping,

$$\gamma_{i\sigma,j\sigma} = i\sigma t_{\rm so}\sin(\phi_i-\phi_j), \quad (19)$$

where $t_{\rm so}$ is a constant that depends on the distance between the adatom and the graphene sheet. When introducing this hopping and applying the symmetries Eq. (10), we obtain that the coupling between Bloch states of different sublattices and same spin cancels identically. On the contrary the spin-conserving coupling between same sublattice Bloch functions gets a finite value that changes sign when changing spin, sublattice, or Dirac cone,

$$\langle\Psi_{\tau,s,\sigma}|V_H|\Psi_{\tau,s,\sigma}\rangle = \frac{1}{N}3\sqrt{3}t_{\rm so}\sigma s\tau. \quad (20)$$

This term has the same form as the Hamiltonian Eq. (5), and we conclude, in agreement with Ref. [28], that a heavy adatom with electrical active p orbital in a hollow position on top of graphene induces an intrinsiclike SOC.

B. Adatom in top position

In this geometry the adatom is located vertically on top of a carbon atom at a height h. This configuration privileges the sublattice A of the underneath carbon atom. In the top arrangement the carbon p_z orbital is orthogonal to the p_x and p_y orbitals of the adatom located on top of it. Therefore the processes contributing to first neighbor spin-conserving tunneling are zero by symmetry, Eq. (13). However, an adatom on top of a carbon of a given sublattice induces spin-conserving tunneling between carbon atoms of the opposite sublattice,

$$\langle\Psi_{B(A),s,\sigma}|V_{T_{A(B)}}|\Psi_{B(A),s,\sigma}\rangle = \tau_{A(B)}\frac{3\sqrt{3}}{N}t_{\rm so}\sigma s, \quad (21)$$

where $V_{T_{A(B)}}$ represents the perturbation created by the adatom on top of atoms belonging to sublattice $A(B)$. Therefore adatoms in top positions induce intrinsiclike SO coupling, although it is important to note that the sign of this conserving tunneling is opposite to that induced by an adatom in the hollow position, Eq. (20).

Because of the symmetry of the orbitals, only one of the mechanisms described in Eq. (14) contributes to spin-flip tunneling between first neighbors,

$$\gamma_{i\sigma,j-\sigma} = -\sigma t_R e^{-i\sigma\phi_j}, \quad (22)$$

where t_R is a constant that depends on carbon to adatom tunneling parameters. Adding the contributions from the three first neighbors of the underneath C atom, we get the following contribution to the low energy Hamiltonian,

$$\langle\Psi_{A,s,\sigma}|V_{T_{A(B)}}|\Psi_{B,s,-\sigma}\rangle = \frac{1}{N}3t_R s\frac{(1+\sigma s)}{2}. \quad (23)$$

This Rashba-like SOC has the same form and sign independently on the sublattice where the adatom is placed. The Rashba term gets its origin in the broken mirror symmetry produced by the adatoms, and this is reflected in that t_R changes sign depending on whether the top adatoms are located on the top or bottom of the graphene layer.

VI. NUMERICAL RESULTS

Adatoms deposited on graphene should be placed at minimum energy equilibrium positions. The adsorption geometry depends on the particular heavy adatom [28], being one of the more interesting in that the adatoms place in hollow positions. When the adatoms are intercalated between graphene and the substrate, the adatoms form a superlattice commensurate with the graphene honeycomb lattice [18]. It is also plausible to expect that low energy injected adatoms become deposited in random positions.

In this section we show numerical results of the electronic structure of graphene doped with heavy outer shell p-orbital adatoms in three particular cases: (i) the adatoms are randomly distributed in hollow positions, (ii) the adatoms form a commensurate supercell with the graphene lattice, and (iii) the adatoms are fully randomly distributed on the graphene sheet. In the numerical calculations, we consider a periodic rectangular graphene supercell of dimensions $L_x = N_x\sqrt{3}a$ and $L_y = N_y a$, defined by the lattice vectors $\mathbf{A} = N_y\mathbf{a}$ and $\mathbf{B} = N_x(2\mathbf{b} - \mathbf{a})$. In these expressions, N_x and N_y are integer numbers. The unit cell contains $4N_xN_y$ carbon atoms located at the graphene lattice positions $\{\mathbf{R}_i + \mathbf{d}_\alpha\}$. The adatoms are located at positions $\{\mathbf{r}_i\}$. The concentration of adatoms, x, is given by the ratio of the number of adatoms to the number of carbon atoms.

The electronic structure is obtained by diagonalizing the Hamiltonian,

$$H = H_0 + \sum_{i,j,\sigma,\sigma'} \gamma_{i\sigma,j\sigma'}(|Z,i,\sigma\rangle\langle Z,j,\sigma'| + \text{H.c.}), \qquad (24)$$

where H_0 is the pristine graphene Hamiltonian, Eq. (1), and the second term describes the adatom induced hopping between carbon atoms. Because of the periodic boundary conditions, the electronic structure is described using Bloch's theorem, so that the electronic states are characterized by a band index and wave vectors k_x and k_y that are defined in the interval $[-\frac{\pi}{L_x}, \frac{\pi}{L_x}]$ and $[-\frac{\pi}{L_y}, \frac{\pi}{L_y}]$, respectively. In this geometry and for N_y not being a multiple of three, the Dirac cones occur at wave vectors $\mathbf{K} = (\mathbf{0}, \frac{2\pi}{3\mathbf{L_y}})$ and $\mathbf{K}' = (\mathbf{0}, \frac{4\pi}{3\mathbf{L_y}})$. For N_y being a multiple of three, the two Dirac cones overlap at the Γ point. This overlap does not imply coupling between electronic states in different Dirac cones, provided the adatoms are randomly distributed in the supercell [31]. In order to simplify the analysis of the results, in this work we always consider supercells with no overlapping Dirac cones.

Recent experiments seems to indicate that Pb on graphene can induce a large SOC, therefore in the numerical calculations we chose Pb as the adatom, and we use the tight-binding parameters obtained in Ref. [18] for Pb atoms on graphene, $h = 0.27$ nm, $V_{pp\sigma}(h) = 0.4$ eV, $V_{pp\pi}(h) = -0.6$ eV, $\epsilon_x = \epsilon_y = 1.65$ eV, $\epsilon_z = 1.38$ eV, $\Delta_{SO} = 0.9$ eV, and $t = 2.7$ eV.

A. Adatoms in hollow positions

In this subsection we analyze supercells with different sizes and forms and with different concentrations of adatoms randomly distributed but always located in hollow positions. In Fig. 3 we show an example of supercell of size $N_x = 5$, $N_y = 7$ with 17 adatoms deposited in a random way in hollow positions. In the inset of Fig. 4 we plot a typical band structure obtained for an adatom concentration $x = 0.25$. The adatoms open a gap at the Dirac points and, in agreement with the results presented in Sec. V A, the band structure corresponds to a Dirac equation in the presence of an intrinsic SOC, Eqs. (4) and (5). In our numerical calculations we obtain that for adatoms adsorbed in hollow positions, and for the parameters corresponding to Pb, the band structures for different adatom configurations are practically the same, independent of supercell size and form. Therefore there is not dispersion in the value of the energy gap obtained in the numerical simulations. In our numerical calculations we obtain that for atoms adsorbed in hollow positions, the band structure always has this form, independent of supercell size and form

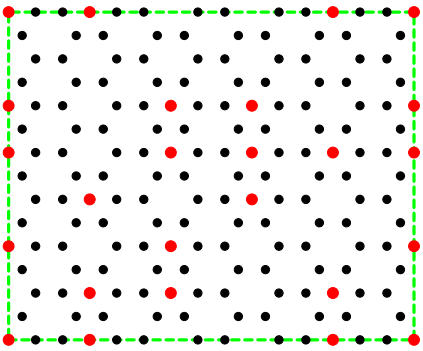

FIG. 3. (Color online) Graphene supercell with $N_x = 5$ and $N_y = 7$. Black small circles represent carbon atoms. Larger red circles indicate the position of the adatoms. The adatoms are located in hollow positions, and in this figure we plot a particular random realization of disorder. In this figure the number of adatoms per carbon atoms is $x = 17/140$.

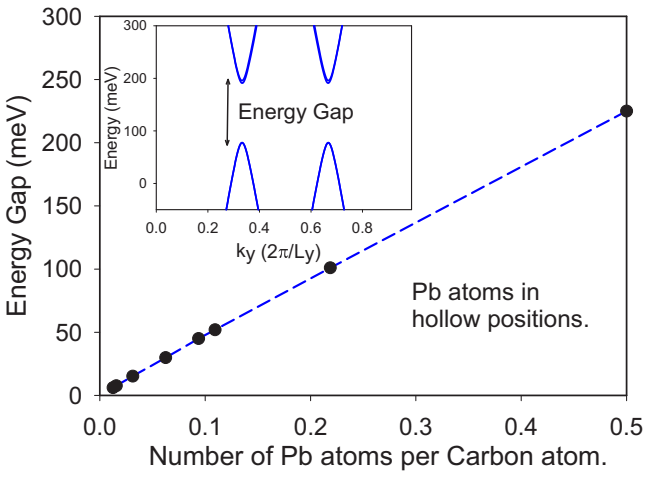

FIG. 4. (Color online) In the inset we plot a band structure of a rectangular graphene supercell with $x = 0.25$ Pb atoms per carbon. The Pb adatoms induce a gap at the Dirac points $(0, \frac{2\pi}{3L_x})$ and $(0, \frac{4\pi}{3L_x})$. As commented on in the text, the band structure is practically independent of the supercell size, and the gap only depends on the concentration of Pb atoms. In the main figure we plot the gap at the Dirac points as a function of the Pb atoms' concentration. The parameters used in the calculations are taken from Ref. [18].

or disorder realization. The SOC depends only on the heavy atoms' concentration. In Fig. 4 we plot the energy gap as a function of the adatom concentration x.

Using Green function techniques we infer that the linear dependence of the gap with the density of adatoms implies a negligible interference between adatoms. The low energy properties of an electron are described by the Dirac equation $\hbar v_F \sigma_0 (s k_x \tau_x + k_y \tau_y)$, and the corresponding Green function is

$$G_0(\mathbf{k},\omega) = \frac{1}{\hbar\omega - H_0} = \frac{\sigma_0}{\hbar\omega^2 - \hbar v_F^2 k^2} \begin{pmatrix} \omega & v_F k e^{i\theta_{\mathbf{k}}} \\ v_F k e^{-i\theta_{\mathbf{k}}} & \omega \end{pmatrix}. \quad (25)$$

Here $\theta_{\mathbf{k}} = \tan^{-1} \frac{k_y}{s k_x}$. An adatom located in a hollow position, at $\mathbf{r}_i$, produces a scattering potential of the form $s\sigma_z\tau_z\delta(\mathbf{r} - \mathbf{r_i})$. In the presence of a density x of adatoms in hollow positions and neglecting multiple scattering, the Green function of the total Hamiltonian is [32]

$$G(\mathbf{k},\omega) = G_0(\mathbf{k},\omega) + x\Delta s\sigma_z G_0(\mathbf{k},\omega)\tau_z G(\mathbf{k},\omega). \quad (26)$$

Inverting this equation we get

$$G(\mathbf{k},\omega) = \frac{1}{\hbar^2\omega^2 - \hbar^2 v_F^2 k^2 - x^2\Delta^2} \times \begin{pmatrix} \hbar\omega + x\Delta s\sigma_z & \hbar v_F k e^{i\theta_{\mathbf{k}}} \\ \hbar v_F k e^{-i\theta_{\mathbf{k}}} & \hbar\omega - x\Delta s\sigma_z \end{pmatrix} \quad (27)$$

that corresponds to the virtual crystal Hamiltonian $H = H_0 + x\Delta s\sigma_z\tau_z$, describing graphene in the presence of an intrinsic SOC of magnitude $x\Delta$.

B. Commensurate array of Pb atoms on graphene

Graphene grown on Ir(111) forms a 9.3×9.3 moiré superstructure with a ~25 Å periodicity [33]. When Pb atoms are intercalated under the graphene monolayer, the Pb atoms form a rectangular lattice commensurate with Ir. Therefore the honeycomb graphene lattice and the array of Pb atoms commensurate in a large moiré supercell [18].

In this subsection we study the spin-orbit effects induced by a rectangular array of Pb atoms of dimensions $l_x \times l_y$ commensurate with a large rectangular graphene supercell of dimensions $L_x \times L_y$, see Fig. 5(a). In the inset of Fig. 5(b) we plot, for the geometry shown in Fig. 5(a), the electronic states obtained with the tight-binding parameters corresponding to Pb. The band structure coincides with the eigenvalues of the Dirac equation in the presence of a Rashba-like spin-orbit coupling. The intensity of the SO coupling is proportional to the energy gap between the second conduction band and the second valence band. We find that this gap increases linearly with the Pb concentration x and only depends on the concentration of Pb atoms being independent of geometrical details. In Fig. 5(b) we plot the energy gap as a function of x for a graphene supercell characterized by $N_x = 10$ and $N_y = 5$ and different combination of i_x and i_y. We obtain the same linear dependence for larger graphene supercells.

These results indicate that Rashba couplings induced from different adatoms do not interfere, and the total Rashba coupling is just the sum of the different contributions. The Rashba SO coupling induced by Pb adatoms always have the same sign, dictated by the broken mirror symmetry, and the linear behavior reveals that in the commensurate phase, the adatoms average all possible locations in the graphene unit cell. On the contrary, the absence of a gap at the Dirac points indicates that the contribution to intrinsic SOC from adatoms located in different places sums zero. This occurs because the sign of the intrinsic SOC induced by adatoms depends on its location. A particular example is the case of the intrinsic SOC induced by adatoms in the hollow position, Eq. (20), that has opposite sign from that induced by adatoms located in the top positions, Eq. (21).

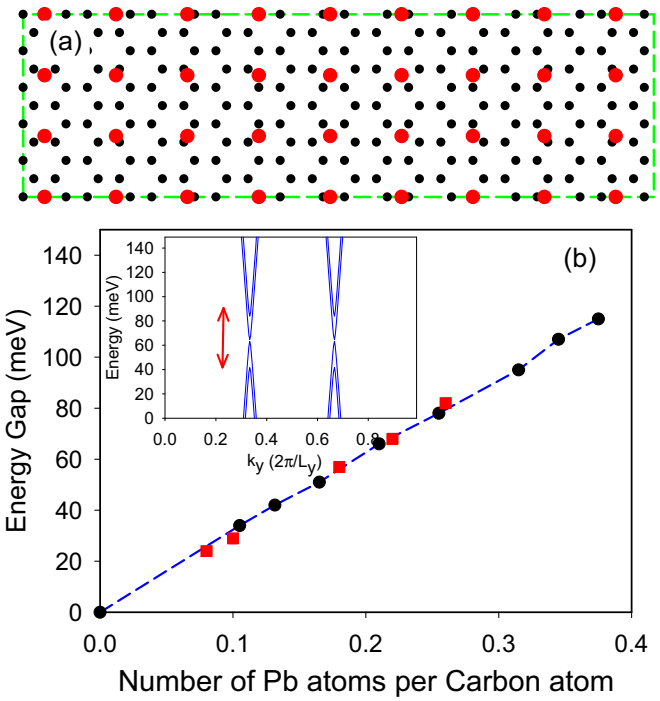

FIG. 5. (Color online) (a) Graphene supercell with $L_x = 10\sqrt{3}a$ and $L_y = 5a$. Black small circles correspond to the positions of the carbon atoms. Larger red circles represent adatoms. The adatoms form a rectangular lattice commensurate with the graphene supercell. In the figure the dimensions of the adatom cell are $l_x = L_x/9$ and $l_y = L_y/3$. (b) Inset: band structure for the geometry presented in (a). Main figure: dependence of the energy gap, as defined in the inset, as a function of the Pb atoms' concentration. Black points are obtained in the graphene supercell fixing the dimension $l_y = L_y/3$ and changing l_x. Red points are obtained fixing $l_x = L_x/9$ and changing l_y. The parameters used in the calculation are taken from Ref. [18].

C. Random positions

Finally we compute the SO induced in graphene by a concentration of Pb adatoms randomly distributed. We study large graphene unit cells, Fig. 6(a), with different concentrations of adatoms. The main results of the simulations are that there is not a band gap at the Dirac points of the band structure, Fig. 6(b), and the Rashba-like SOC increases linearly with the concentration of Pb atoms, Fig. 6. These results are independent of the disorder realization and size and form of

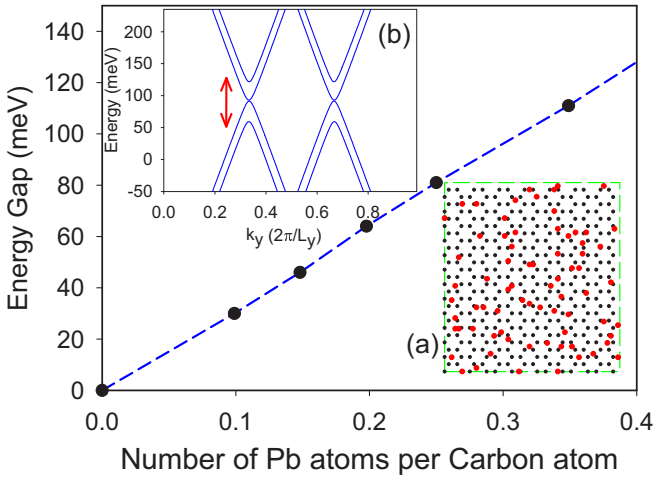

FIG. 6. (Color online) (a) Graphene supercell with $L_x = 7\sqrt{3}a$ and $L_y = 13a$. Black small circles correspond to the positions of the carbon atoms. Larger red circles represent adatoms. The concentration of adatoms is $x = 0.2$, and they are located in a random way. (b) Inset: band structure for the geometry presented in (a). Main figure: dependence of the energy gap, as defined in the inset, as a function of the Pb atoms' concentration. The energy gap only depends on Pb concentration and is independent of geometry or disorder realization. The parameters used in the calculation are taken from Ref. [18].

the unit cell. The dependence of the SOC on Pb concentration is the same as in the case of commensurate supercell. This, and the absence of intrinsiclike SOC, indicate that in both cases, commensurate order and random positions, there are not interference effects between adatoms, and the resulting SOC is just the sum of the contributions from adatoms placed in different positions.

VII. TOPOLOGICAL PROPERTIES

In the previous sections we have obtained that a graphene layer doped with adatoms placed in hollow positions has a gapped energy band structure similar to that obtained from the Dirac equation with an intrinsic SOC. On the contrary, adatoms randomly or commensurately distributed on graphene generate a gapless band structure that remind us of graphene with Rashba SOC. In this section we check that both adsorption geometries, hollow and random, have the same topological properties of the Dirac equation plus intrinsic and Rashba SOC, respectively. In order to know the topological properties, we compute the spin-resolved Hall conductivity of the system,

$$\sigma_{xy}^{\sigma} = -2 \sum_{n,n',\mathbf{k}} \frac{\mathrm{Im}(\langle n\mathbf{k}|v_x \hat{P}_\sigma |n'\mathbf{k}\rangle \langle n'\mathbf{k}|v_y \hat{P}_\sigma |n\mathbf{k}\rangle)}{(\varepsilon_{n,\mathbf{k}} - \varepsilon_{n',\mathbf{k}})^2}, \qquad (28)$$

where $|n\mathbf{k}\rangle$ and $\varepsilon_{n\mathbf{k}}$ are the eigenfunction and eigenvectors, respectively, of the supercell Hamiltonian Eq. (24); in the sum the index n and n' run over occupied and empty states, respectively, $v_\nu = -\frac{1}{\hbar}\frac{\partial H}{\partial k_\sigma}$ is the velocity operator in the ν direction, and $\hat{P}_\sigma$ projects the wave function in the subspace of spin σ.

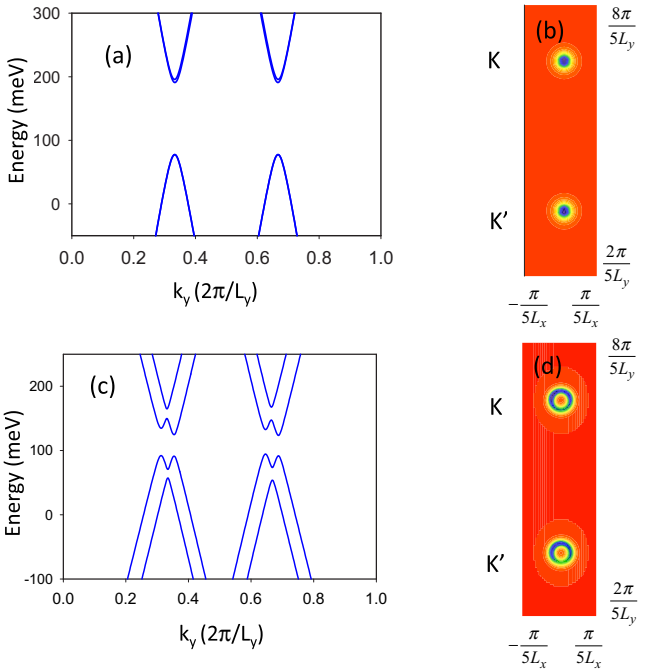

FIG. 7. (Color online) (a) Band structure of a graphene supercell ($N_x = 5$, $N_y = 7$) with a concentration $x = 0.25$ of adatoms randomly located in hollow positions. (b) Partial section of the Brillouin zone showing in green the regions that contribute to the spin-up Hall conductivity $\sigma_{xy}^{\uparrow}$ for the case in (a). (c) Same as (a) for a fully random distribution of adatoms and an exchange field of 18 meV. (d) Partial section of the Brillouin zone showing in green the regions that contribute to the total Hall conductivity $\sigma_{xy}^{\uparrow} + \sigma_{xy}^{\downarrow}$ for the case in (c).

In the case of adatoms in hollow positions, we have obtained

$$\sigma_{xy}^{\sigma} = \sigma \frac{e^2}{h}$$

adatoms in hollow positions; that corresponds to a quantum spin-Hall system [7]. The total Hall conductivity sums zero, as it should be in a system with time reversal symmetry. The main contributions to the Hall conductivity come from circular regions centered at the Dirac points, Figs. 7(a) and 7(b).

Adatoms placed randomly on graphene do not generate a gap in the band structure, and the Hall conductivity is zero. However, in Refs. [11] and [12], it was proposed that an exchange field applied to graphene in the presence of Rashba SOC should open a gap, and the system would be a nontrivial insulator characterized by a quantized anomalous Hall effect. We have applied a uniform exchange field to the randomly doped graphene, and we have obtained a gapped band structure, Fig. 7(c), and a finite Hall conductivity

$$\sigma_{xy} = \sigma_{xy}^{\uparrow} + \sigma_{xy}^{\downarrow} = 2\frac{e^2}{h}$$

that proves that adatoms placed randomly on graphene generate a Rashba SOC. In this case, and because of the form of the bands, Fig. 7(c), the main contributions to the Hall conductivity come from annulus centered at the Dirac points, Fig. 7(d). The realization of the quantum spin-Hall effect and quantum anomalous Hall effect for hollow and random

adatoms, respectively, shows the stability of these topological phases even for a nonuniform distribution of the adatoms.

VIII. SUMMARY

In this paper we have studied the spin-orbit coupling induced in graphene by heavy adatoms with active electrons residing in p orbitals. Depending on the location of the adatoms, we find different induced SOC's. Adatoms located in hollow positions open a gap at the Dirac points and induce an intrinsiclike SOC. However adatoms randomly placed or commensurate with the graphene lattice maintain the system gapless and induce a Rashba-like SOC. The adatoms only perturb the pristine graphene band structure near the Dirac points.

We find that the SOC induced by the adatoms is additive, and there are not interference effects or multiple scattering. The topological properties of graphene with hollow or random adatoms are the same as those of the Dirac Hamiltonian in the presence of intrinsic or Rashba SOC, respectively. The finite value of the Hall conductivity of graphene doped in different geometries indicates the robustness of the topological phases against a nonuniform distribution of the spin-orbit coupling.

ACKNOWLEDGMENT

This work has been supported by MEC-Spain under Grant No. FIS2012-33521.

[1] A. H. Castro Neto, F. Guinea, N. M. R. Peres, K. S. Novoselov, and A. K. Geim, Rev. Mod. Phys. **81**, 109 (2009).
[2] M. I. Katsnelson, *Graphene: Carbon in Two Dimensions* (Cambridge University Press, Cambridge, 2012).
[3] D. Huertas-Hernando, F. Guinea, and A. Brataas, Phys. Rev. B **74**, 155426 (2006).
[4] H. Min, J. E. Hill, N. A. Sinitsyn, B. R. Sahu, L. Kleinman, and A. H. MacDonald, Phys. Rev. B **74**, 165310 (2006).
[5] B. Dlubak, M.-B. Martin, C. Deranlot, B. Servet, S. Xavier, R. Mattana, M. Sprinkle, C. Berger, W. A. De Heer, F. Petroff, A. Anane, P. Seneor, and A. Fert, Nat. Phys. **8**, 557 (2012).
[6] L. Chico, A. Latge, and L. Brey, Phys. Chem. Chem. Phys. **17**, 16469 (2015).
[7] C. L. Kane and E. J. Mele, Phys. Rev. Lett. **95**, 226801 (2005).
[8] M. Z. Hasan and C. L. Kane, Rev. Mod. Phys. **82**, 3045 (2010).
[9] X.-L. Qi and S.-C. Zhang, Rev. Mod. Phys. **83**, 1057 (2011).
[10] E. Prada, P. San-Jose, L. Brey, and H. Fertig, Solid State Commun. **151**, 1075 (2011).
[11] Z. Qiao, S. A. Yang, W. Feng, W.-K. Tse, J. Ding, Y. Yao, J. Wang, and Q. Niu, Phys. Rev. B **82**, 161414 (2010).
[12] W.-K. Tse, Z. Qiao, Y. Yao, A. H. MacDonald, and Q. Niu, Phys. Rev. B **83**, 155447 (2011).
[13] A. H. Castro Neto and F. Guinea, Phys. Rev. Lett. **103**, 026804 (2009).
[14] S. Abdelouahed, A. Ernst, J. Henk, I. V. Maznichenko, and I. Mertig, Phys. Rev. B **82**, 125424 (2010).
[15] L. Chico, M. P. López-Sancho, and M. C. Muñoz, Phys. Rev. B **79**, 235423 (2009).
[16] D. Gosálbez-Martinez, J. J. Palacios, and J. Fernández-Rossier, Phys. Rev. B **83**, 115436 (2011).
[17] J. Balakrishnan, G. Kok Wai Koon, M. Jaiswal, A. H. Castro Neto, and B. Ozyilmaz, Nat. Phys. **9**, 284 (2013).
[18] F. Calleja, H. Ochoa, M. Garnica, S. Barja, J. J. Navarro, A. Black, M. M. Otrokov, E. V. Chulkov, A. Arnau, A. L. Vazquez de Parga, F. Guinea, and R. Miranda, Nat. Phys. **11**, 43 (2015).
[19] A. Avsar, J. Y. Tan, T. Taychatanapat, J. Balakrishnan, G. K. W. Koon, Y. Yeo, J. Lahiri, A. Carvalho, A. S. Rodin, E. C. T. O'Farrell, G. Eda, A. H. Castro Neto, and B. Özyilmaz, Nat. Commun. **5**, 4875 (2014).
[20] A. Pachoud, A. Ferreira, B. Özyilmaz, and A. H. Castro Neto, Phys. Rev. B **90**, 035444 (2014).
[21] A. Ferreira, T. G. Rappoport, M. A. Cazalilla, and A. H. Castro Neto, Phys. Rev. Lett. **112**, 066601 (2014).
[22] H. Yang, C. Huang, H. Ochoa, and M. A. Cazalilla, arXiv:1510.07771.
[23] D. Marchenko, A. Varykhalov, M. R. Scholz, G. Bihlmayer, E. I. Rashba, A. Rybkin, A. M. Shikin, and O. Rader, Nat. Commun. **3**, 1232 (2012).
[24] J. Balakrishnan, G. K. W. Koon, A. Avsar, Y. Ho, J. H. Lee, M. Jaiswal, S.-J. Baeck, J.-H. Ahn, A. Ferreira, M. A. Cazalilla, A. H. C. Neto, and B. Özyilmaz, Nat. Commun. **5**, 4748 (2014).
[25] M. Gmitra, D. Kochan, and J. Fabian, Phys. Rev. Lett. **110**, 246602 (2013).
[26] S. Irmer, T. Frank, S. Putz, M. Gmitra, D. Kochan, and J. Fabian, Phys. Rev. B **91**, 115141 (2015).
[27] R. M. Guzmán-Arellano, A. D. Hernández-Nieves, C. A. Balseiro, and G. Usaj, Phys. Rev. B **91**, 195408 (2015).
[28] C. Weeks, J. Hu, J. Alicea, M. Franz, and R. Wu, Phys. Rev. X **1**, 021001 (2011).
[29] M. Zarea and N. Sandler, Phys. Rev. B **79**, 165442 (2009).
[30] E. Suárez Morell, P. Vargas, L. Chico, and L. Brey, Phys. Rev. B **84**, 195421 (2011).
[31] H. Jiang, Z. Qiao, H. Liu, J. Shi, and Q. Niu, Phys. Rev. Lett. **109**, 116803 (2012).
[32] E. Economou, *Green's functions in quantum physics* (Springer, Berlin, Heidelberg, New York, 2006).
[33] A. T. N'Diaye, J. Coraux, T. N. Plasa, C. Busse, and T. Michely, New J. Phys. **10**, 043033 (2008).